Received: 10 May 2021 | Revised: 14 October 2021 | Accepted: 23 November 2021

DOI: 10.1002/we.2705

RESEARCH ARTICLE

WILEY

Constrained power reference control for wind turbines

Daniel S. Zalkind | Marco M. Nicotra | Lucy Y. Pao

Department of Electrical, Computer, and Energy Engineering, University of Colorado Boulder, Boulder, Colorado, USA

Correspondence
Daniel S. Zalkind, Department of Electrical, Computer, and Energy Engineering, University of Colorado Boulder, Boulder, CO 80309, USA.
Email: dan.zalkind@gmail.com

Funding information
Advanced Research Projects Agency - Energy (ARPA-E), Grant/Award Number: DE-AR0000667

Abstract

The cost of wind energy can be reduced by controlling the power reference of a turbine to increase energy capture, while maintaining load and generator speed constraints. We apply standard torque and pitch controllers to the direct inputs of the turbine and use their set points to change the power output and reduce generator speed and blade load transients. A power reference controller increases the power output when conditions are safe and decreases it when problematic transient events are expected. Transient generator speeds and blade loads are estimated using a gust measure derived from a wind speed estimate. A hybrid controller decreases the power rating from a maximum allowable power. Compared to a baseline controller, with a constant power reference, the proposed controller results in generator speeds and blade loads that do not exceed the original limits, increases tower fore-aft damage equivalent loads by 1%, and increases the annual energy production by 5%.

KEYWORDS
condition monitoring, design constraints, extreme event control, power boost, power control, transient estimation, wind energy

1 | INTRODUCTION

Typical wind turbine controllers regulate the generator speed, either for optimal power capture in below-rated operation or to ensure safe generator speeds in above-rated operation. Designs with these goals result in controllers with adequate and robust enough performance to be ubiquitous as a baseline, but they do not reflect the overall design goals of a wind turbine.

For offshore turbines, with larger capital and balance-of-station costs than onshore turbines, the primary factor to reduce the cost of wind energy is increasing energy capture.[1] However, most recent research in wind turbine controls is aimed at reducing structural loading on the turbine, which could (a) result in blades that are designed to be lighter if the control design is considered during the blade design or (b) enable longer lasting structures. Based on recent studies, a 25% reduction in blade mass results in a 2.5% reduction in the levelized cost of energy (LCOE),[2] whereas increasing the annual energy production (AEP) by 10% can result in nearly a 10% decrease in the LCOE.[3]

When designing the hardware components of a turbine, structural loads are calculated using standard simulations and either fatigue or the worst-case extreme loads from these simulations are used to design the various turbine components; they are referred to as design-driving loads. Thus, structural loading on a turbine behaves like a constraint on the design, especially for large, modern rotors, where extreme, or peak, loading drives design. In two recent system-level design analyses for turbines with blades around 100 m in length, peak loads during extreme turbulence were found to drive blade design.[2,4]

Because power capture is directly related to the cost of energy and structural loading acts like a constraint on design, we design a controller to increase power capture while maintaining the same load and generator speed limits. Generator speed also behaves like a constraint; when a certain threshold is exceeded, supervisory control initiates a shutdown procedure, which reduces the turbine's availability and ultimately its net

AEP. However, the standard approach to controlling generator speed is still based on regulating the speed to a constant set point, while ensuring that there is an adequate margin between that set point and the shutdown threshold.

We implement our controller using methods similar to the standard, regulator-based control approaches[5–7] because they are indicative of methods widely used in the field. We then add control modules that change the set points and limits of those controllers to achieve our goal of increasing power capture and reducing blade loads. This modular design approach (shown in Figure 1) is consistent with realistic, collaborative controller development, as opposed to replacing existing controllers with a single, monolithic control algorithm to accomplish all tasks. A set point controller (SPC) ensures that both the pitch and torque controller are not simultaneously active, while a power controller (PC) uses the minimum pitch angle and rated generator speed to change the power output. Minimum pitch peak shaving (*MPPS* in Figure 1), or "thrust clipping," is widely referred to in wind turbine control reports[6] as a method of reducing the peak loads that occur near-rated wind speeds. These control elements are commonly used in practice, but are often unpublished or in various, fragmented reports. In this article, we present the control laws so that they can all be implemented together by a reader. Other control methods, like individual pitch control and nacelle acceleration feedback, can also be used to reduce structural loads[8]; they can work in parallel to the proposed method but are not included in this article.

In the wind energy industry, controlling generator power is common practice. For example, the power output is reduced (referred to as de-rating or curtailing) for electrical grid support.[9] Boosting the power output has also been marketed by industrial white papers[10,11] for increasing the operator's revenue, though manufacturer's methods remain unpublished.

In this article, we seek an answer to the following question: If we actively control the power reference (PR), rather than maintaining it at a static value, how much can we increase power capture while still maintaining safe operation? An approach, called "envelope protection,"[12] uses an optimal control approach to de-rate the turbine only when some limit, or envelope, is expected to be exceeded. In another approach, power control for reducing peak structural loads was tuned using turbulence statistics and simulation results.[13] Both approaches inspired this work, which we have extended to include power boosting and peak shaving methods, in what we refer to as power reference control (*PRC* in Figure 1). We divide the *PRC* into slow (PRC^0) and transient (PRC^1) PRCs. In PRC^0, the upper limit of the power reference R is determined using a filtered wind speed signal; simulation results guide the design of this component so that power capture is maximized, and generator speed limits are not violated. PRC^1 uses a wind gust measure to estimate transients in the generator speed and blade loads. During the development of this controller, we found that most overspeed and high load events are caused by a similar wind occurrence: when the wind speed first decreases and then increases. The proposed gust measure reflects our desire to control this type of event, while a hybrid control scheme de-rates the turbine when estimated transients are expected to exceed some limit. This hybrid control system[14] makes discrete state transitions between two continuous control schemes: a safe and de-rating controller. To the authors' knowledge, the proposed gust measure, transient estimation, and PRC, with the goal of increasing energy capture, have not been presented in the literature.

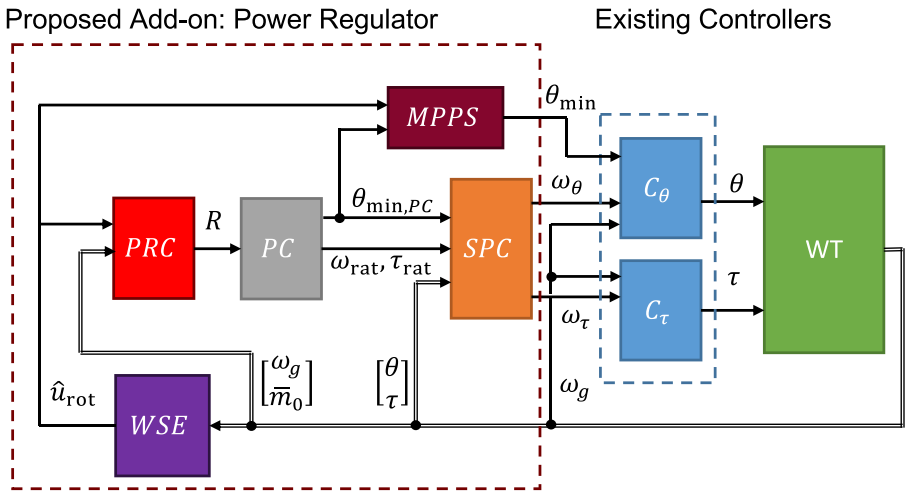

FIGURE 1 High-level schematic of the elements used to control generator power with structural load and generator speed constraints. The rotor average wind speed $\hat{u}_{\text{rot}}$ is estimated (using a wind speed estimator *WSE*) from turbine signals and used along with the generator speed ω_g and filtered collective blade load $\bar{m}_0$ to determine the power reference R in the power reference controller (*PRC*). The power controller (*PC*) determines the minimum pitch for power control $\theta_{\min,PC}$ and rated generator speed ω_{rat} and torque τ_{rat}, while the minimum pitch peak shaver (MPPS) determines the lower pitch limit $\theta_{\min}$ used by the pitch controller C_θ. The set point controller (*SPC*) determines the generator speed set points to the pitch and torque controller (C_τ), ω_θ and ω_τ, respectively. The pitch and torque controllers provide the pitch θ and torque τ inputs to the wind turbine (WT)

Previous versions of this work included more analysis from a control theory perspective, the potential benefits of operating with a known wind input or reduced turbulence, and detailed discussions about the design choices.[15,16] This article presents the control method in its basic form, using a wind speed estimate (WSE) (summarized in Appendix A) for the wind input, in enough detail so that it can be implemented by a wind turbine control designer. We also include a demonstration of the resulting control signals and a summary of the results that can be achieved when using PRC for increasing power and constraining peak generator speeds and blade loads.

The various modules are connected as shown in Figure 1. The measures used to quantify results are presented in Section 2 to familiarize the reader with our design goals and procedures. The open-source wind turbine model is described in Section 3, which is provided pitch and torque inputs (θ and τ, respectively) using the proportional–integral (PI) pitch and torque controllers in Section 4. The set point controller (*SPC*) and *PC* provide generator speed references (ω_θ and ω_τ) given a power reference *R* as described in Section 5, while the minimum pitch peak shaver (*MPPS*) provides the lower pitch limit $\theta_{\min}$ to the PI pitch controller using the method in Section 6. The *PRC* provides the power reference *R* to the lower levels of control in Section 7, using turbine states (generator speed ω_g and filtered collective blade load $\bar{m}_0$) and an estimated wind speed signal ($\hat{u}_{\text{rot}}$). Finally, simulation results of various control configurations are presented in Section 8.

2 | DESIGN MEASURES

We simulate controllers and compare performance in simulation environments specified by a subset of the power producing design load cases (DLCs) determined by the International Electrotechnical Commission[17]:

- DLC 1.2: normal turbulence model (NTM) with six seeds at each mean wind speed from cut-in to cut-out (Table 1), spaced 2 ms^{-1} apart, and
- DLC 1.3: extreme turbulence model (ETM), using the same mean wind speeds and number of seeds.

In practice, other DLCs also affect design loads, but we focus on the power producing cases to demonstrate the trade-off between power production and structural loading.

Generator speed

Because supervisory wind turbine controllers begin a shutdown procedure when the generator speed exceeds some threshold, we have selected 120% of the nominal rated generator speed of 1174 rpm (1408 rpm) as the threshold not to exceed; an example time series and the constraint is shown in Figure 2. Before final implementation, the probability of exceeding the overspeed threshold should be investigated using more simulations and extrapolation methods similar to those used for loads in the IEC standards.[17] Designers would also need to consider that the generator speed limits may be determined by generator and power electronic specifications.

TABLE 1 NREL-5MW reference turbine and environmental parameters

Turbine parameters	Value
Rated power	5 MW
Rated rotor speed	12.1 rpm
Hub height	87 m
Number of blades	3
Rotor radius	63 m
Max chord	4.65 m
Rotor position	Upwind
Precone angle	-2.5°
Baseline gross capacity factor	45.1%
Baseline rated wind speed	11.4 ms^{-1}
Blade mass	17.7 t
Environmental parameters	
Wind turbine site class	Class 1A
Cut-in, cut-out wind speed	5, 25 ms^{-1}
Mean wind speed at 50 m, hub height	7.87, 9.11 ms^{-1}
Weibull shape, scale factor	2.17, 10.3

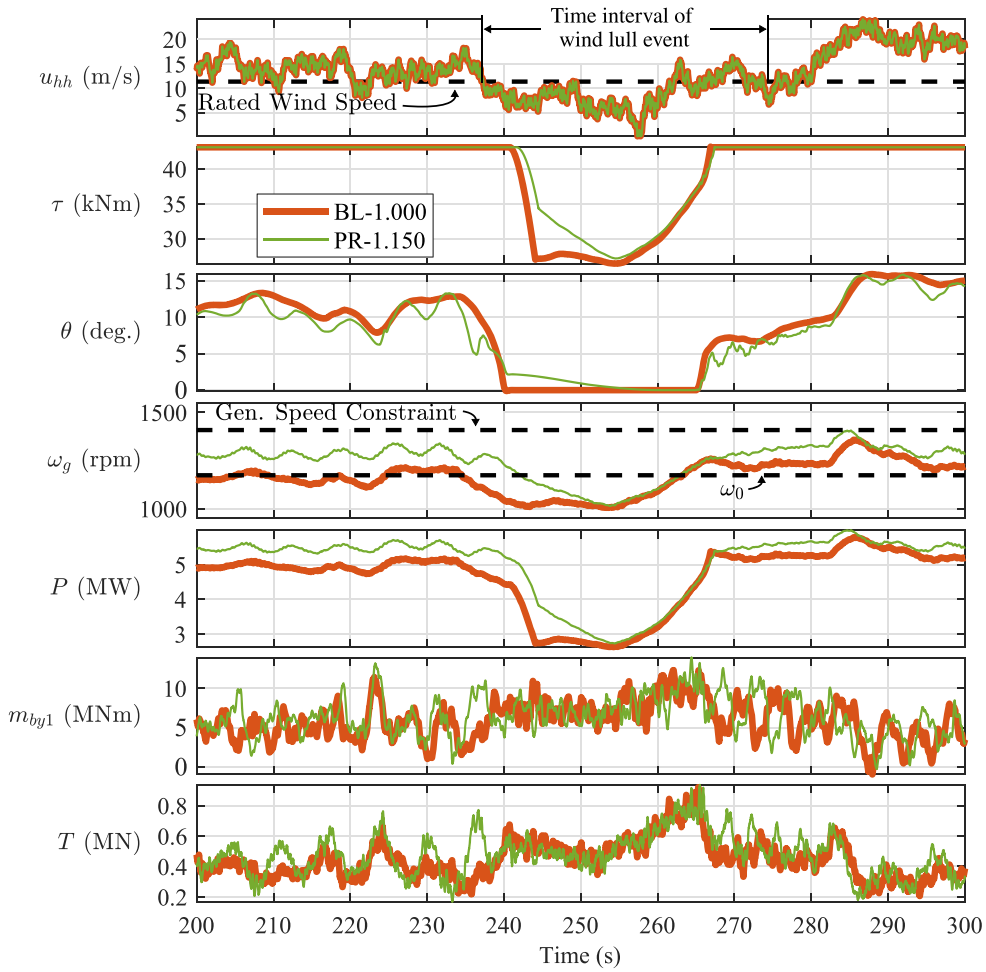

FIGURE 2 Time series of a problematic wind speed lull, where u_{hh}, the hub height wind speed, decreases and then increases from about 240–275 s. The generator torque τ and blade pitch θ control decrease to regulate the generator speed ω_g and power P. Low pitch angles with increasing wind speeds lead to large thrust-based loading on the turbine, as indicated by the thrust T and the blade 1 root bending moment m_{by1} around 265 s. The baseline control (BL-1.000) is designed to regulate the generator speed to a constant ω_0. In this article, we propose a controller (PR-1.150) that varies the power reference so that constraints on the generator speed (and loads) are not exceeded, while increasing the power output during safe operation (e.g., before 240 s and after 290 s)

Extreme blade loads

The blade load that is used to design the structural aspects of a wind turbine blade is referred to as its design load. Some blade designs use the maximum blade load over all DLC simulations to determine the design load.[18] Another measure is the characteristic load: It is the maximum (across wind speeds) of the average maximum load (over the turbulence seeds); it has less randomness than the overall maximum. Blade designers often use the combined (edgewise and flapwise directions) blade load for design, but since the edgewise load is mostly deterministic with the rotor azimuth, the combined load is primarily dependent upon the flapwise load. For this reason, we focus on the flapwise blade design load in this article. Peak blade loads typically occur when the pitch angle is low and wind speed increases, often following a decrease in wind speed; for example, between 240 and 275 s in Figure 2.

Rotor thrust and tower fatigue

Rotor thrust drives tower loading, which is closely related to tower cost.[19] We use the lifetime damage equivalent load (DEL) of the tower base fore-aft (FA) moment to measure the fatigue on the tower; this load tends to increase when the PR is changed due to extra pitch actuation. Load cycles are computed in MLife[20] and extrapolated over the lifetime of the turbine using the wind speed distribution in Table 1. Since rotor thrust and tower loads are closely related to the pitch angle, this measure can also represent the level of pitch actuation. We try to avoid increasing the tower FA DEL by more than 10%.

Energy capture or lifetime average power

The measure with the greatest impact on the cost of wind energy is the AEP. To compute the AEP, the average power of the six turbulent simulations at each mean wind speed are averaged, resulting in a power curve $P(u)$ for each controller, which is weighted so that

$$LAP = \sum_{u \in U} p(u)P(u), \tag{1}$$

where LAP is the lifetime average power and $p(u)$ is the (Weibull) wind speed distribution defined in Table 1. AEP is equal to the value in (1) multiplied by the number of hours in a year; we leave this factor off to give a more intuitive measure of the lifetime average power in MW in the results of Section 8.

Pitch travel

Additional pitch actuation is the primary cost of the control presented in this article. To measure the change in control actuation, we compute the pitch travel at each mean wind speed u

$$\theta_{\text{travel}}(u) = \frac{1}{T_{\text{sim}}} \int |\dot{\theta}| dt, \tag{2}$$

where the pitch travel is normalized by the simulation length T_{sim}, and we weigh the pitch travel by the wind speed distribution:

$$\theta_{\text{travel}}^{\text{Life}} = \sum_{u \in U} p(u)\theta_{\text{travel}}(u), \tag{3}$$

to compute the lifetime average pitch travel per second.

3 | WIND TURBINE MODEL

We simulate the NREL-5MW reference turbine,[21] summarized in Table 1, using OpenFAST[22] with wind fields generated using TurbSim[23] according to the design Class 1A. The environmental conditions have a significant effect on the power capture and structural fatigue (via the wind speed distribution). We have chosen to simulate in an environment that represents an offshore site on the east coast of the United States. A project developer would ultimately decide the turbulence class (A, B, or C) based on the environment. We have chosen the greatest amount of turbulence (Class 1A) to demonstrate the de-rating controller, though lower turbulence, with fewer large wind lull events, might result in even greater power gains.

Increasing the rated generator speed through control actions increases both the capacity factor and the wind speed at which the rated generator power is reached (rated wind speed), while decreasing the rated generator speed has the opposite effect. In Table 1, we show the nominal values without power regulation. Using the wind speed distribution in Table 1 without power regulation results in a capacity factor of 45.1%; this capacity factor is less than more recently developed turbines, which have larger rotors relative to the rated generator power. However, this turbine represents a realistic case for using the power boosting functionality presented in this article as an aftermarket addition to existing infrastructure.

4 | PI TORQUE AND PITCH CONTROL

To control the direct inputs to the wind turbine, torque τ, and pitch θ, we use PI controllers (Figure 3), which are commonly used control architectures, both in research and industry, and we would like to maintain their use when designing the other control modules.

4.1 | Pitch control

The pitch controller is a gain-scheduled PI control. Because the magnitude of the sensitivity of power to pitch angle decreases as the pitch increases,[21] the PI gains of the pitch controller should decrease to maintain consistent generator speed regulation. The gain-correction factor, GK

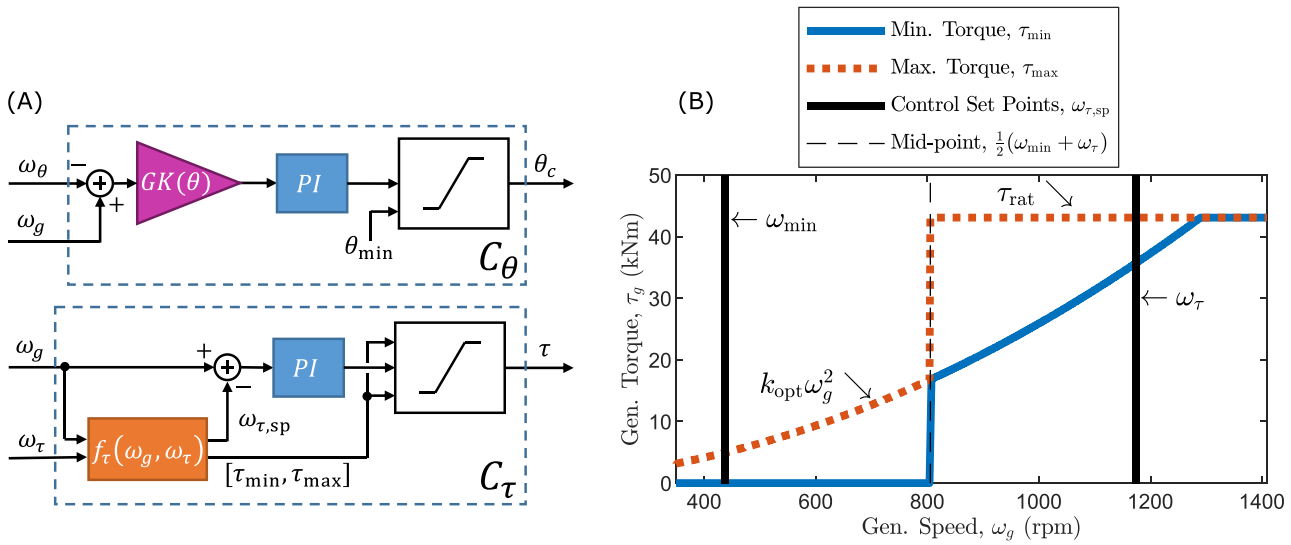

FIGURE 3 PI control modules (A) provide the torque τ and pitch θ controls to the wind turbine, subject to upper and lower limits on torque and pitch. Note that θ_c is the commanded pitch input to the pitch actuator, θ is the current pitch angle of the blades, and $GK(\theta)$ is a gain scheduling parameter. The nonlinear function $f_\tau(\omega_g, \omega_\tau)$ given in (4) is visualized in (B), which determines the generator speed set point $\omega_{\tau,\text{sp}}$ and torque saturation limits $[\tau_{\min}, \tau_{\max}]$, depending on whether the generator speed is near cut-in or rated operation. Anti-windup schemes are necessary for each integrator in the proportional–integral (PI) controllers, which are both active at all times, but may be saturated

TABLE 2 Parameters for proportional–integral pitch and torque controllers

	Parameter	Variable	Value
Turbine parameters	Total drivetrain inertia	J_{tot}	4.38×10^7 kg m^2
	Minimum gen. speed	$\omega_{\min}$	436.5 rpm
	Nominal rated gen. speed	ω_0	1174 rpm
	Gearbox ratio	G	97
Pitch control parameters	Gain scheduling param.	θ_k	4.71°
	Pitch regulator mode: natural frequency	$\omega_{\text{reg},\theta}$	0.275 rad s^{-1}
	Pitch regulator mode: damping ratio	$\zeta_{\text{reg},\theta}$	1.59[a]
	Pitch regulator: proportional gain	$k_{P,\theta}$	0.0143 s
	Pitch regulator: integral gain	$k_{I,\theta}$	7.18×10^{-4}
Torque control parameters	Optimal torque control gain	k_{opt}	0.22 N·m rpm^{-2}
	Torque regulator: proportional gain	$k_{P,\tau}$	9.75 N·m s rad^{-1}
	Torque regulator: integral gain	$k_{I,\tau}$	4.88 N·m rad^{-1}

[a]A damping ratio greater than 1 results in two real poles, rather than two complex conjugate poles.

(θ) in Figure 3A, is applied to the generator speed error, rather than to the gains themselves for a simpler anti-windup implementation and to maintain appropriate gains throughout above-rated wind speeds.[24]

The PI gains $k_{P,\theta}$ and $k_{I,\theta}$ in Table 2 are determined using the desired natural frequency (or bandwidth) $\omega_{\text{reg},\theta}$ and the damping ratio $\zeta_{\text{reg},\theta}$ of the generator speed regulator mode.[21] Increasing the bandwidth $\omega_{\text{reg},\theta}$ results in a faster pitch response to wind disturbances and better generator speed regulation, but also greater structural loading. We determine the regulator mode using a data-driven optimization procedure with the goal of reducing fatigue loads on the tower, such that no maximum generator speed transients exceed 120% of the nominal rated generator speed.[25] Since the worst-case generator overspeed occurs during an ETM simulation with a 20 ms^{-1} mean wind speed (Figure 12), that wind input is used to tune the parameters of the pitch controller. The optimization procedure results in a regulator mode with a lower bandwidth and higher damping ratio than the prescribed values originally recommended for this rotor and pitch controller.[21] The reduced bandwidth is also beneficial when the pitch control set point is changed using the transient PRC (Section 7.3.1). The pitch command θ_c is filtered using a second-order butterworth filter with a cutoff frequency of 1 Hz, which represents the pitch actuator, to determine the pitch θ of the turbine.

The pitch control set point ω_θ is normally the nominal rated generator speed (ω_0=1174 rpm), but we control this value to increase power capture or decrease generator speed transients, by increasing or decreasing ω_θ, respectively. The minimum pitch setting $\theta_{\min}$ is usually the optimal pitch angle of the blades with respect to energy capture, but we control this value to change the power output in Section 7.1 and reduce peak blade loading in Section 6.

4.2 | Torque control

We implement a PI torque controller similar to previous work,[6,8] which provides a smoother torque control and a simpler implementation than lookup-table-based control schemes if we change the rated generator speed. The torque control gains $k_{P,\tau}$ and $k_{I,\tau}$ in Table 2 are derived using a similar approach to the pitch control gains by defining a "regulator mode" of the torque controller, which has been tuned to balance energy capture with power fluctuations.[16]

Depending on whether the turbine is near cut-in or rated operation, the generator speed set point $\omega_{\tau,\text{sp}}$ and torque limits $[\tau_{\min}, \tau_{\max}]$ are changed using the nonlinear function

$$[\omega_{\tau,\text{sp}}, \tau_{\min}, \tau_{\max}]^T = f_\tau(\omega_g, \omega_\tau) = \begin{cases} [\omega_{\min}, 0, k_{\text{opt}}\omega_g^2] & \text{if } \omega_g < \frac{1}{2}(\omega_{\min} + \omega_\tau), \\ [\omega_\tau, k_{\text{opt}}\omega_g^2, \tau_{\text{rat}}] & \text{otherwise,} \end{cases} \tag{4}$$

where ω_τ is the generator speed set point for the torque controller, ω_g is the generator speed, and τ_{rat} is the rated generator torque; (4) is illustrated in Figure 3.

5 | SET POINT AND POWER CONTROL

5.1 | Set point control

To ensure that both torque and pitch are not simultaneously controlling the generator speed, we use an SPC developed by Sowento.[26] If both PI torque and pitch controllers have the same generator speed set points, both will be active, leading to poor performance in terms of power production and increased pitch actuation, which increases the loading on the turbine.

The SPC module, shown in Figure 4, uses a generator speed set point bias,

$$\delta\omega_g = \text{LPF}_{10}\{g_1(\theta - \theta_{\min,PC}) - g_2(\tau_{\text{rat}} - \tau)\}, \tag{5}$$

where the gains g_1 and g_2 are both positive and LPF_{10} is a low-pass filter

$$\text{LPF}_{\tau_l} = \frac{(2\pi/\tau_l)^2}{s^2 + \left(2\pi\sqrt{2}/\tau_l\right)s + (2\pi/\tau_l)^2}, \tag{6}$$

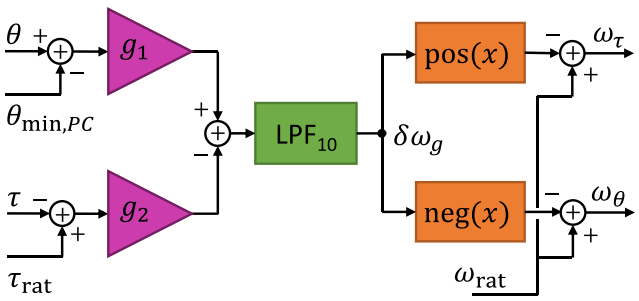

FIGURE 4 Set point smoothing control used to determine generator speed set points ω_θ and ω_τ for PI control in Figure 3, given the current pitch angle θ, the minimum pitch setting for power control $\theta_{\min,PC}$, torque τ, rated torque τ_{rat}, and rated generator speed ω_{rat}

where $\tau_l = 10\,\text{s}$ and $s = j\omega$ is the complex frequency; τ_l was chosen to ensure a smooth $\delta\omega_g$ signal. The set point bias is applied to the torque and pitch set points, depending upon the sign of $\delta\omega_g$:

$$\omega_\tau = \begin{cases} \omega_{\text{rat}} - \delta\omega_g & \text{if } \delta\omega_g > 0 \\ \omega_{\text{rat}} & \text{otherwise} \end{cases} \tag{7}$$

and

$$\omega_\theta = \begin{cases} \omega_{\text{rat}} - \delta\omega_g & \text{if } \delta\omega_g < 0 \\ \omega_{\text{rat}} & \text{otherwise,} \end{cases} \tag{8}$$

which is related to whether the turbine is in above- or below-rated operation. Typically, $\delta\omega_g > 0$ during above-rated operation and vice versa. The nonlinear functions in (7) and (8) are represented in the block diagram in Figure 4, where

$$\text{pos}(x) = \begin{cases} x & \text{if } x > 0 \\ 0 & \text{otherwise} \end{cases} \tag{9}$$

and

$$\text{neg}(x) = \begin{cases} x & \text{if } x < 0 \\ 0 & \text{otherwise.} \end{cases} \tag{10}$$

During above-rated operation, $\theta > \theta_{\text{min},PC}$, which increases $\delta\omega_g$ and reduces ω_τ in (7), biasing the torque control towards rated torque τ_{rat}. During below-rated operation, $\tau < \tau_{\text{rat}}$, reducing $\delta\omega_g$, which, if negative, increases ω_θ in (8) and biases the pitch control towards its minimum saturation limit $\theta_{\text{min},PC}$. The design choices for the gains in this controller are shown in Table 3, and they are tuned based on the power capture and power variation of near-rated simulations.[16]

5.2 | Power controller

To change the power output of the turbine, the rated generator speed is controlled so that

$$\omega_{\text{rat}} = R\omega_0, \tag{11}$$

where ω_0 is the original rated generator speed (1174 rpm) and R is the PR factor; this works across all operating wind speeds.

To de-rate the turbine in below-rated operation, the minimum pitch setting is controlled using $\theta_{\text{min},PC} = f_{PC}(R)$, which, along with the minimum pitch peak shaver in Section 6, contributes to the saturation limit used by the PI pitch controller. With a minimum pitch setting greater than the optimal (or fine) pitch setting θ_{fine}, the aerodynamic torque and generator speed are reduced. The function $f_{PC}(R)$ that determines the minimum pitch setting is shown in Figure 5B; it is determined using simulations with a below-rated, constant wind inflow by varying the minimum pitch angle, finding the power output compared to the optimal output, and inverting the function.[16]

We cannot always increase power output above the rated value. However, we can always de-rate the turbine, which is desirable whenever a problematic gust event occurs. Going forward, we use the control architecture described to this point, with $R = 1$, as a baseline for comparison.

TABLE 3 Set point and power control parameters

	Parameter	Variable	Value
Turbine	Rated gen. torque	τ_{rat}	43.1 kNm
Parameters	Fine pitch angle	θ_{fine}	0°
Set point control	Torque set point bias	g_1	33.3 rpm deg.$^{-1}$
Design choices	Pitch set point bias	g_2	2.79 rpm (kNm)$^{-1}$

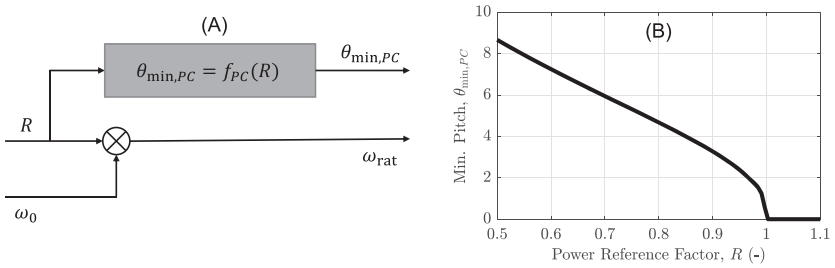

FIGURE 5 The power controller (A), given a power reference factor R, sets the minimum pitch angle $\theta_{\min,PC}$ according to $f_{PC}(R)$ as shown in (B) and the rated generator speed ω_{rat}

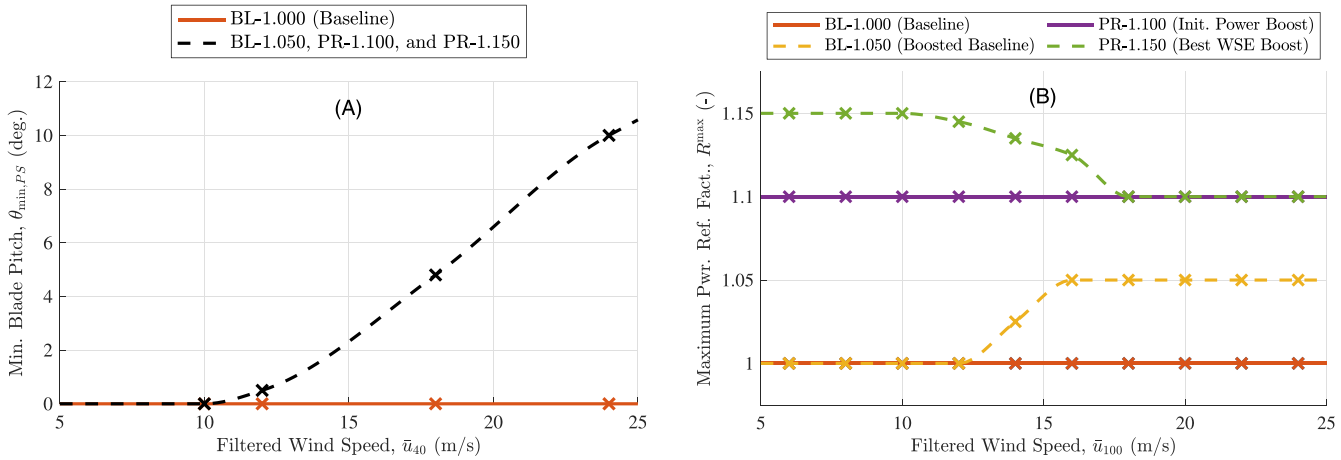

FIGURE 6 Minimum pitch peak shaving control (A) and maximum power reference factor (B) for the various control cases described in Section 8

6 | PEAK SHAVING USING MINIMUM PITCH CONTROL

The goal of the MPPS controller is to prevent instances where there is a low pitch angle and high wind speed, causing a large torque and thrust on the rotor. In the simulations performed using the previously described controller (with a constant PR factor of $R = 1$), this occurs during wind lulls at high wind speeds. The MPPS control determines the lower limit on the pitch command (Figure 3A):

$$\theta_{\min} = \max\{\theta_{\min,PC}, \theta_{\min,PS}\}, \tag{12}$$

where $\theta_{\min,PC}$ is the minimum pitch setting for power control (Section 5.2) and $\theta_{\min,PS}$ is the minimum pitch for peak shaving.

A lookup table defines the function $\theta_{\min,PS}(\bar{u}_{40})$, which depends on the slow low-pass filtered WSE $\bar{u}_{40} = \text{LPF}_{40}\{\hat{u}_{\text{rot}}\}$, where LPF_{τ_l} is defined in (6). A τ_l of 40 s ensures that the minimum pitch signal does not change too rapidly, introducing dynamics in near-rated wind speeds and that there is some memory of the mean wind speed, so that when problematic wind lulls occur, the minimum pitch value is still high enough to avoid large rotor thrusts. Between the breakpoints in Figure 6A, cubic interpolation determines $\theta_{\min,PS}$. We use a break point at 10 ms^{-1}, just below rated, such that $\theta_{\min,PS}(10) = \theta_{\text{fine}}$. The minimum blade pitch $\theta_{\min,PS}$ at 12 ms^{-1}, just above the rated wind speed, is tuned to trade-off power capture and peak loading.[25] The minimum pitch angles at the high wind speed breakpoints (18 and 24 ms^{-1}) are chosen so that the lookup table is always non-decreasing, and peak blade loads across DLC 1.3 are less than the peak loads at 12 ms^{-1}.

7 | POWER REFERENCE CONTROL

Sections 4–6 have described control elements that can be found elsewhere in the literature,[6,8,21] which we have adapted to more easily accept changing generator speed set points so that they work with the PRC described in the following. The PRC (Figure 7) is designed to reduce the PR factor R when a critical performance variable (structural loading or generator speed) is predicted to exceed a pre-defined

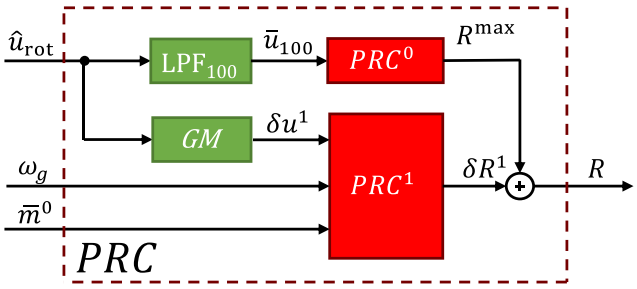

FIGURE 7 The power reference controller, which uses the estimated wind speed $\hat{u}_{\mathrm{rot}}$, generator speed ω_g, and filtered collective blade load $\bar{m}^0$ as inputs; the output is the power reference factor R. The slow power reference control (PRC^0) uses a low-pass filtered wind speed ($\bar{u}_{100}$) to determine the maximum power reference $R_{\max}$, which is decreased (by the magnitude of δR^1, which is always negative) when problematic transients are expected, estimated using the gust measure (GM) δu^1

threshold. Otherwise, R is increased to produce more energy. Because the wind, turbine, and controller behave differently across wind speeds, we use a filtered wind speed signal to determine the maximum allowable PR factor $R^{\max}$ using the slow PRC (PRC^0) described in Section 7.1. To de-rate the turbine during transient events ($R < R^{\max}$), we use information about the change in wind speed and turbine measurements to decrease R using the transient PRC (PRC^1), a hybrid control system detailed in Section 7.2. The stability of the PRC is discussed in Section 7.3, along with an analysis of its steady-state behavior and disturbance rejection properties. A demonstration is presented in Section 7.4.

7.1 | Slow power reference control

In the slow PRC (PRC^0), we control the maximum power reference factor $R^{\max}$ based on a slow low-pass filtered wind speed $\bar{u}_{100} = \mathrm{LPF}_{100}\{\hat{u}_{\mathrm{rot}}\}$, where LPF_{τ_l} is defined in (6). A time constant of $\tau_l = 100\,\mathrm{s}$ ensures that the maximum power reference factor does not introduce dynamics that would affect the stability of the closed-loop system; this is discussed in more detail in Section 7.3.1. For the NREL-5MW turbine and the previously described control modules, at wind speeds near cut-out, larger gusts result in greater generator speed transients, so we reduce $R^{\max}$ at high wind speeds (18–24 ms^{-1}) to reduce the average and maximum generator speeds. Different lookup tables are shown in Figure 6B: We place breakpoints 2 ms^{-1} apart and ensure a smooth interpolation using a cubic interpolation. $R^{\max}$ (shown in Figure 8D) is then the upper bound on the power reference factor R used by the PC in Section 5.2.

Increasing $R^{\max}$ increases the average power, but also peak generator speeds. Since increasing $R > 1$ results in a lower pitch angle for the same wind speed compared to $R = 1$, thrust-based loading is also increased. The design choice for $R^{\max}$ versus $\bar{u}_{100}$ (Figure 6B) is ultimately up to the control designer. Here, we outline the method used to arrive at the lookup tables that produce the results of Section 8. Since maximum generator speeds depend on the fast PRC (PRC^1), presented in Section 7.2, it is important to note that we tune the PRC^0 module only after the PRC^1 is implemented. Any changes to PRC^1 may require re-tuning PRC^0.

After PRC^1 is implemented, we perform the following procedure:

1. Simulate DLC 1.3 and find the worst generator speed maxima case
2. Increase $R^{\max}$ across wind speeds until the generator constraint is violated
3. Re-simulate DLC 1.3 and repeat the process, increasing $R^{\max}$ at wind speeds where there is a gap between the maximum generator speed and the upper bound (see, e.g., the difference between PR-1.100 and PR-1.150 in Figure 6B and the corresponding maximum generator speeds in Figure 12B).
4. If the constraint is violated, find the $\bar{u}_{100}$ when the maximum occurs and reduce $R^{\max}$ at the closest breakpoint(s) until the constraint is not violated.

7.2 | Transient PRC

In the transient PRC (PRC^1), we predict peaks in the generator speed and blade loads that occur due to wind speed changes, and then de-rate the turbine during these events. In this article, we use a WSE $\hat{u}_{\mathrm{rot}}$. In previous work, we demonstrated how perfect wind speed measurements could improve control performance.[16] The other inputs to PRC^1 are generator speed ω_g, a known and measurable quantity, and a filtered estimate of

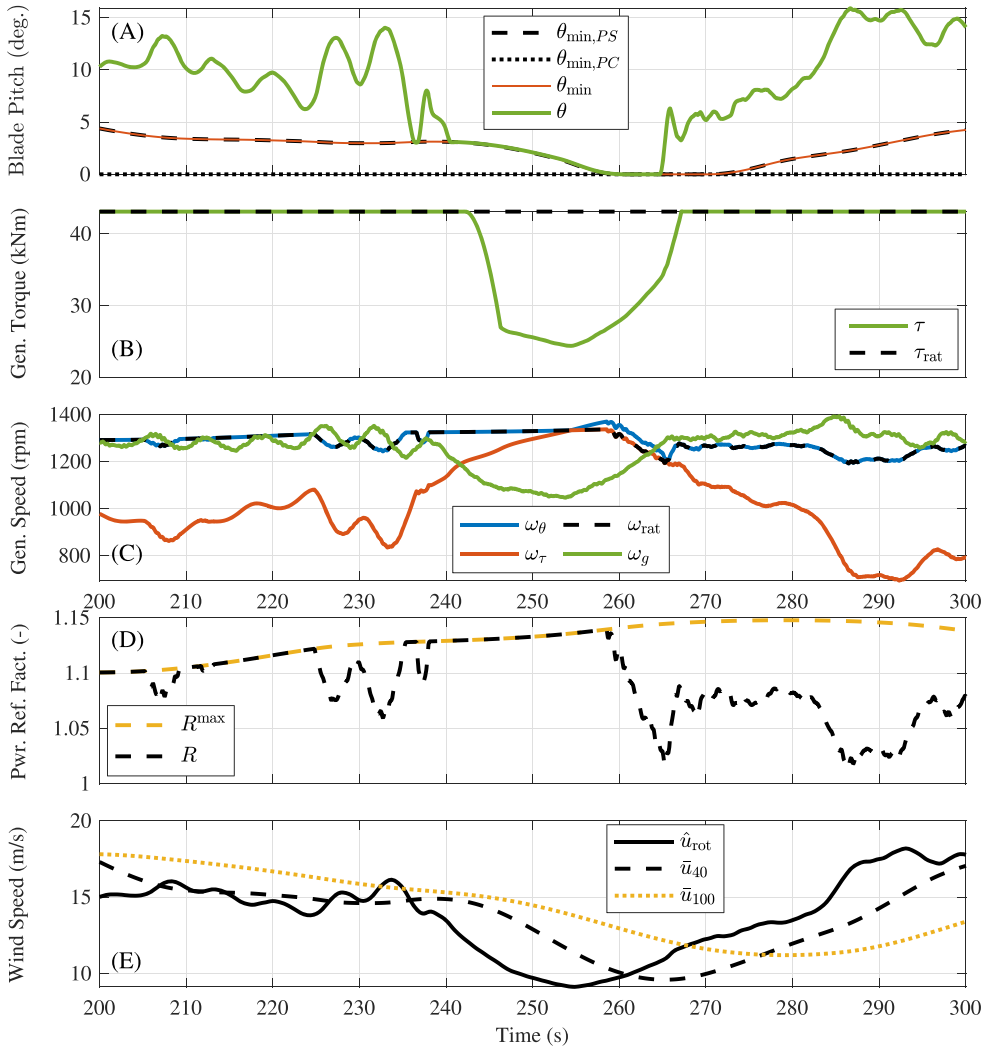

FIGURE 8 Demonstration of the pitch and torque PI controllers (Section 4 and Figure 3), set point control (Figure 4), power control (Figure 5), minimum pitch peak shaving (Section 6 and Figure 6A), and slow power reference control (Figure 6B). The generator speed ω_g is controlled with the blade pitch θ, generator torque τ, and the set points, ω_θ and ω_τ, which depend on the rated generator speed ω_{rat} and set point smoothing controller in Section 5.1. The torque and pitch are saturated by τ_{rat} and $\theta_{\min}$, respectively. The pitch control generator speed set point ω_θ is increased from the rated generator speed ω_{rat} when the torque τ is less than rated torque τ_{rat} so that the blade pitch is biased towards the minimum pitch setting $\theta_{\min}$. The torque control generator speed set point ω_τ decreases when the blade pitch θ is greater than the minimum pitch setting $\theta_{\min,PC}$, which biases the torque control towards its maximum rated torque. The rated generator speed $\omega_{\text{rat}} = R\omega_0$, where ω_0 is the nominal rated generator speed. A wind speed estimate $\hat{u}_{\text{rot}}$ is low-pass filtered ($\bar{u}_{40}$ and $\bar{u}_{100}$) and used as the inputs to lookup tables that determine the minimum pitch setting for peak shaving $\theta_{\min,PS}$ and the maximum power reference factor $R^{\max}$ (an upper bound on R). The minimum pitch limit $\theta_{\min}$ used by the PI pitch controller is defined in (12). Since the power reference factor $R > 1$ for this timeseries, the minimum pitch for power control $\theta_{\min,PC} = 0°$, the optimal pitch angle for this rotor

the collective blade load component $\bar{m}^0$, which is found by taking the average of the three blade load signals and filtering the signal to eliminate the polluting harmonic frequencies:

$$\bar{m}^0 = \mathcal{F}\left\{\frac{1}{3}(m_{by,1} + m_{by,2} + m_{by,3})\right\}, \tag{13}$$

where $m_{by,i}$ is the flapwise blade load of blade i and $\mathcal{F}$ is a filter designed to eliminate the polluting harmonic from the collective blade load signal. The filter

$$\mathcal{F} = \text{NF}_{3P}(s, \omega_{3P}) \times \text{LPF}_1(s), \tag{14}$$

includes a low-pass filter as in (6), with a time constant of 1 s, and a moving notch filter

$$\mathrm{NF}(s,\omega_{3P}) = \frac{s^2 + 2\omega_{3P}\beta_{3P}s + \omega_{3P}^2}{s^2 + 2\omega_{3P}\zeta_{3P}s + \omega_{3P}^2}, \tag{15}$$

that depends on the changing 3P rotor frequency

$$\omega_{3P} = \mathrm{LPF}_{100}\left\{\frac{3\omega_g}{G}\right\}, \tag{16}$$

which requires a slow low-pass filtered generator speed for stability and $G = 97$ is the gearbox ratio of the NREL-5MW reference turbine.[21] The parameters (Table 4) of the notch filter (ζ_{3P}, β_{3P}) are tuned to reduce the 3P oscillations in the load signal.

7.2.1 | Gust measure

Given the generator speed and blade load, we use information about the wind disturbance to estimate transient changes in those signals. An extended Kalman filter (EKF) is used to estimate the rotor average wind speed. The blade pitch, generator torque, and generator speed measurements are inputs to the EKF.[16] Peak generator speeds and blade loads often occur during lulls in the wind that are followed by increasing wind speeds; we refer to this type of event, shown in Figures 2 and 9A, as a "negative gust." Our goal is to detect this type of event with a high level of reliability.

First, we sample past wind speeds using multiple delays:

$$U_r = \hat{u}_{\mathrm{rot}}(t - t_r), \tag{17}$$

where $r = \{0, 1, 2, \ldots, N_d\}$ and the different delays

$$t_r = r\Delta t_d \tag{18}$$

are spaced Δt_d seconds apart. The difference between the current wind speed and the set of delayed wind speeds

$$\Delta U_r = w_r[\hat{u}_{\mathrm{rot}}(t) - \hat{u}_{\mathrm{rot}}(t - t_r)] \tag{19}$$

is weighted, giving a greater contribution to wind speed increases that occur in a shorter amount of time:

$$w_r = \frac{1 - w_0}{t_{N_d}} t_r + w_0, \tag{20}$$

TABLE 4 Parameters of the transient power regulator, *PRC*[1], where ω_0 is the nominal rated generator speed, shown in Table 2

	Parameters	Variable	Value
Blade load	Notch filter width	ζ_{3P}	1
Filter parameters	Notch filter depth	β_{3P}	0.1
Gust measure	Delay interval	Δt_d	1 s
	Number of delays	N_d	20
	Gust weighting	w_0	2.5
Transient estimation	Gen. speed gain	d_ω	40 rpm/(ms^{-1})
	Load gain	d_m	750 kNm/(ms^{-1})
	Overspeed gain	k_ω	$0.5/\omega_0$
Transient de-rating	Overload gain	k_m	3×10^{-5} (kNm)$^{-1}$
	Overspeed limit	ω^{Lim}	1325 rpm
	Overload limit	m^{Lim}	9×10^3 kNm

which is shown in Figure 9C, where w_0 is the weight applied to the zero-delayed wind speed difference. Sharp increases in the wind speed have a larger effect on transients, and we can account for this using w_r. The maximum ΔU_r

$$\delta u^1 = \max_{r=0,1,2,\ldots,N_d} \{\Delta U_r\} \tag{21}$$

is the gust measure used to predict transients in the generator speed and blade loads. The process is illustrated in Figure 9 and implemented in Simulink[27] with a user-defined function and a buffer of the past $N_d \times \Delta t_d$ seconds of the wind speed signal. When determining the parameters of the gust measure, shown in Table 4, the overall goal is to align large values of δu^1 with peaks in the generator speed.[16]

The definition of the gust measure ensures that $\delta u^1 \geq 0$, since the difference between the current wind speed and itself is included in the set $\{\Delta U_r\}$. The choice of N_d is a trade-off between reducing computational complexity and ensuring that gusts are detected starting from the minimum of a wind speed lull, for example, near 255 s in Figure 9A,B. If only a single delay were used, the increase in wind speed that occurs from 255 to 265 s would not be registered, and the estimated overspeed would be delayed.

7.2.2 | Transient estimation

We use the gust measure δu^1 to estimate transients in the generator speed and blade loads:

$$\begin{aligned} \hat{\omega} &= \omega_g + d_\omega \delta u^1 \\ \hat{m} &= \bar{m}^0 + d_m \delta u^1, \end{aligned} \tag{22}$$

where d_ω and d_m are positive transient gains for generator speed and blade load, respectively. An example of these signals is shown in Figure 11. The transient gains (in Table 4) are tuned by analyzing the step response to a system only controlled by the PI torque and pitch controllers. For example, if a step in wind speed with a magnitude of $\delta u^1 = 6$ m s^{-1} results in a maximum generator speed of 1400 rpm when the initial speed is 1000 rpm, $d_\omega = (1400 - 1000)/6$.

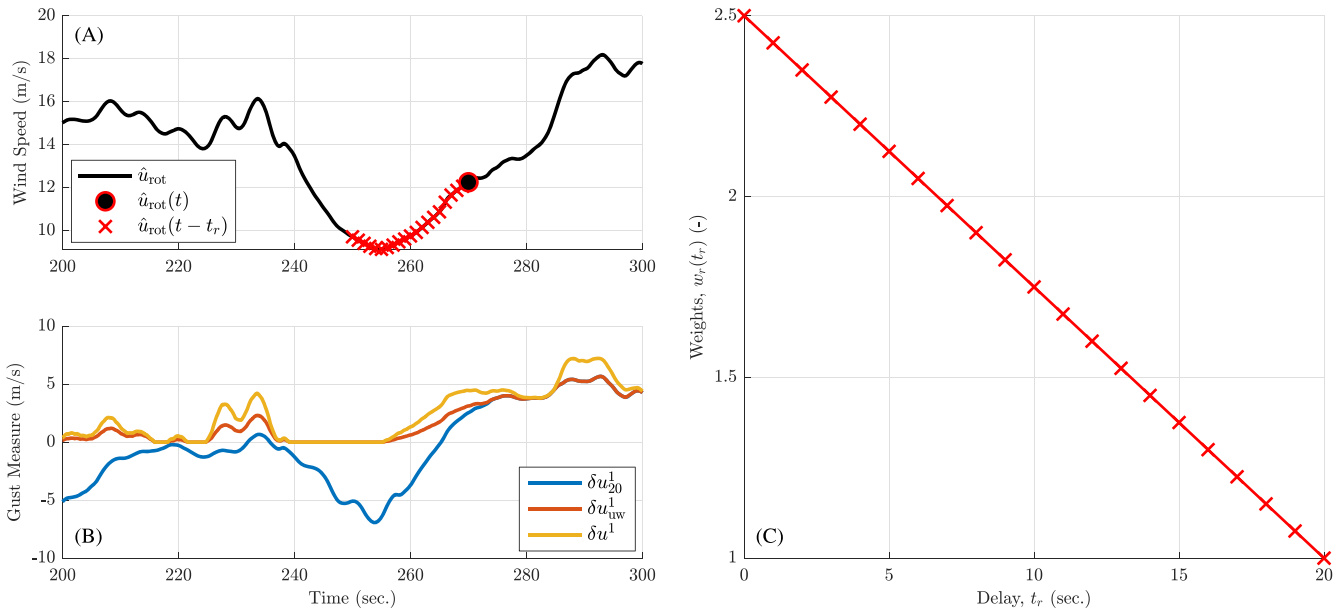

FIGURE 9 The wind speed estimate $\hat{u}_{\text{rot}}$ sampled at time t and at different delays t_r in the past are used to determine the gust measure (A). Three options are presented (B): a single delay (δu^1_{20}), with $t_r = \{20\}$, multiple delays (δu^1_{uw}, un-weighted with $w_0 = 1$ and $t_r = \{0, 1, 2, \ldots, 20\}$), and multiple delays with the same t_r, but weighted with $w_0 = 2.5$ (C) so that wind speed increases that occur quickly have a greater contribution to the gust measure. The wind gust measure δu^1 is used to estimate transients for the controller in this article

More sophisticated methods for estimating transients surely exist, for example, using model predictive control. However, these methods rely on using accurate models, require more computational effort, and make analyzing their behavior more difficult. The goal of this article is to provide a proof-of-concept demonstration for safely increasing the power output using PRC. Improved accuracy of the transient estimation might lead to a more ideal control method, but it is not crucial because de-rating the turbine ultimately leads to safe operation within load and generator speed limits.

7.2.3 | De-rating using a hybrid automata

When the estimated transients $\hat{\omega}$ or $\hat{m}$ exceed thresholds ω^{Lim} and m^{Lim}, respectively, the transient PRC PRC^1 reduces the PR factor so that $R < R^{\max}$. Otherwise, the controller acts as it normally would, with $R = R^{\max}$, to capture as much power as possible. This controller can be implemented as a hybrid automata[14] with two control states: safe and de-rating (Figure 10). The amount of de-rating for each signal of interest x:

$$\delta R_x^1 = -k_x\left(\hat{x} - x^{\text{Lim}}\right), \text{ where } x = \{\omega, m\} \text{ and } k_x > 0 \tag{24}$$

is computed simultaneously for both the generator speed and blade load. To ensure no constraints are violated, the PR factor is reduced by the signal with the greatest amount of de-rating:

$$R = R^{\max}(\bar{u}_{100}) + \min\{\delta R_\omega^1, \delta R_m^1\}, \tag{25}$$

where $R^{\max}(\bar{u}_{100})$ is shown in Figure 6B for several cases and R is the input to the PC in Section 5.2.

7.3 | Power reference control analysis

For analysis purposes, each state in the hybrid system can be modeled separately, while we seek to answer the following questions about the power reference control:

- Stability: Under what conditions are each of the states (safe and de-rating) stable? Is the transition between the states stable?
- Disturbance rejection: Given the system parameters, can we predict the maximum transients that will occur when using the power regulator?
- Steady state: Does the system return to the safe state after a problematic transient event?

Until this point, we have presented the nonlinear control system that is used in DLC simulations. To answer the above questions, we analyze linear models that represent the two states (safe and de-rating) and include the rotor dynamics, pitch actuator, and PI pitch control system, with a wind disturbance ($\hat{u}_{\text{rot}}$) and generator speed reference (ω_θ) inputs. We ignore the nonlinear aspects of the set point controller in Section 5.1 and assume $\omega_\theta = \omega_{\text{rat}}$. We then compare properties found in the hybrid linear system with nonlinear simulation results to verify the closed-loop behavior of the system[16]; the results are summarized next.

7.3.1 | Stability analysis

A thorough stability analysis of this controller is performed using a linear representation of the closed-loop system. The observations in the linear system are supported by nonlinear aeroelastic simulation results; when the linear system is unstable, the nonlinear system is oscillatory.[16]

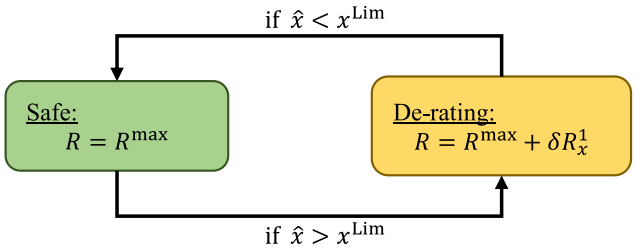

FIGURE 10 State machine for the de-rating signal

Stability of safe state

In the safe state, the reference $R = R^{\max}(\bar{u}_{100})$ varies slowly, since $\bar{u}_{100}$ is a filtered wind speed with a time constant of 100 s. Thus, we assume that $\omega_\theta = R\omega_0$ is constant, and we determine the stability margins of the underlying system, without reference control. The linearized system suggests that there is an upper bound on the pitch control gains, $k_{P,\theta}$ and $k_{I,\theta}$, for the system to be stable. If we use a gain factor G_{fact} to increase both PI gains from their originally designed value in Table 2, such that

$$k_{P,\theta}^{\text{new}} = G_{\text{fact}} k_{P,\theta} \text{ and } k_{I,\theta}^{\text{new}} = G_{\text{fact}} k_{I,\theta}, \tag{26}$$

we will find some $G_{\text{fact}} > 1$ that makes the linear system unstable. In nonlinear simulations, we can determine the gain factor at which the system is unstable by analyzing the tower base fore-aft damage equivalent loading, which is a good indicator of undesirable, extra pitch actuation.[16]

Stability of the de-rating state

When $\hat{\omega} > \omega^{\text{Lim}}$, the turbine is de-rated according to

$$\omega_\theta = \omega_0 \left[R^{\max} - k_\omega \left(\hat{\omega} - \omega^{\text{Lim}} \right) \right]. \tag{27}$$

The linearized change in generator speed

$$\delta\omega_\theta = -k_\omega \omega_0 \omega_g - k_\omega \omega_0 d_\omega \delta u^1 \tag{28}$$

is determined using the generator speed transient in (22). If the linearized PI pitch control dynamics of the safe state are defined as

$$\delta\theta_c = k_{P,\theta}(\omega_g - \delta\omega_\theta) + e_I,\ \dot{e}_I = k_{I,\theta}(\omega_g - \delta\omega_\theta), \tag{29}$$

substituting (28) into (29) shows that the second term in (28) functions like a feedforward input and the first term alters the state dynamics due to its dependence on ω_g. When the system is in the de-rating state, the state dynamics are as if the PI gains are increased by a factor of $(1 + k_\omega \omega_0)$. The gain factor G_{fact} that causes the safe state to be unstable provides an upper bound constraint for stability on the overspeed gain k_ω:

$$k_\omega \omega_0 + 1 < G_{\text{fact}}. \tag{30}$$

De-rating due to load ($\hat{m} > m^{\text{Lim}}$) results in similar, but less intuitive, state dynamics and an upper bound on k_m.

Stability of transition

Since each state of the hybrid system is stable, there must exist a valid Lyapunov function $V = \mathbf{x}^T \mathbf{P} \mathbf{x}$, where $\mathbf{x}$ are the states of the nonlinear system, $\mathbf{P}$ is a positive definite matrix, and the derivative $\dot{V}(\mathbf{x}) = \frac{\partial V}{\partial t} < 0$.[28] Since we can also find a Lyapunov function that works for both the safe and de-rated state using a linear matrix inequality, the states of the hybrid system are always decreasing, regardless of any transitions, which implies that the hybrid system is also stable. The common Lyapunov function can be used as a measure of how close the states converge to an equilibrium point. Using nonlinear simulations, we observe that values of G_{fact} and k_ω that cause unstable linear systems result in nonlinear states that do not converge nearly as closely to the equilibrium points as stable parameters.[16]

7.3.2 | Disturbance rejection

When operating in the de-rating state, the first term of (28) has the effect of increasing the PI gains by a factor of $(1 + k_\omega \omega_0)$, which increases the bandwidth of the closed-loop system and reduces the peak transient in generator speed during a disturbance input. The second term functions as a "feedforward," where the generator speed reference ω_θ is reduced in proportion to the estimated disturbance δu^1 and induces an offset in ω_g. Both effects, the increase in bandwidth and reduction in reference, act to reduce the peak transients when k_ω is increased.

Simulation results also suggest that maximum generator speeds decrease with an increasing k_ω, but only up until some point; there are several reasons why this may occur. There is a delay between the actual wind speed disturbance and wind speed estimate, which propagates to the estimated generator speed transients and de-rating of the turbine, reducing performance in terms of peak generator speed reduction. Additionally, increasing k_ω by too much reduces the stability margin and leads to poor performance in general; extra pitch actuation increases loads and generator speed variation. Generally, it is difficult to control the response to gusts consistently because varied turbine states and random wind speed disturbances make controlling peak generator speeds with a high level of certainty difficult in a realistic operating environment.

7.3.3 | Steady-state analysis

When the controller is in the de-rating state, we want the system to return to the safe state when the problematic wind disturbance has passed, so that the greatest amount of energy is captured. An analysis of the linear models suggests that the steady-state behavior of the de-rating state returns the system to the safe state.[16] Here, we present a logical argument for the system returning to the safe state.

Because the PI pitch (and torque) controllers include integral control, the generator speed will match the set point, $\omega_g \to \omega_\theta$, eventually. When the system is in the de-rating state, the set point is less than the maximum allowable generator speed and the limit that transitions the system into the de-rating state, that is,

$$\omega_\theta < \omega_0 R^{\max} < \omega^{\text{Lim}}. \tag{31}$$

Thus, with enough time for the integral control to act, the generator speed will be less than the transition limit ($\omega_g < \omega^{\text{Lim}}$), and the system will return to the safe state. If the designer chooses an $R_{\max}$ such that (31) is not true and $\omega^{\text{Lim}} < \omega_0 R^{\max}$, then the system will remain in the de-rating state and diminishing benefits in energy capture will occur.

7.4 | Demonstration

Throughout this article, we referred to Figure 2, where a problematic gust event occurs during extreme turbulence with a mean wind speed of 18 ms^{-1}. The controller transitions between above- and below-rated operation during this event and the power drops to nearly half of the rated value. When the wind speed increases, then blade and tower loads peak, as does the generator speed.

The *PRC* determines the gust measure ($\delta u^{\,1}$ in Figure 9), which is used to estimate the generator speed and blade load transients and de-rate the turbine (Figure 11). The maximum PR $R^{\max}$ is determined using the slow low-pass filtered wind speed ($\bar{u}_{100}$) as shown in Figure 8E along with the minimum pitch limit for peak shaving.

The PC uses the power reference R to determine the rated generator speed ω_{rat} and minimum pitch setting for power control $\theta_{\min,PC}$, as shown in Figure 8A, C, and D. The set point smoothing controller determines the set points for the torque and pitch controllers, ω_τ and ω_θ, respectively, which regulate the generator speed ω_g using the torque τ and pitch θ inputs to the turbine (Figure 8A–C). Besides controlling the generator speed, the torque and pitch inputs determine the generator power P, shown in Figure 2, along with the blade load $m_{by,1}$ and rotor thrust T. Several similar events like the one in this demonstration occur when simulating a full set of DLCs, which we report on in Section 8.

8 | SIMULATION RESULTS

Next, we compare controllers using modules common in practice (described in Sections 4–6) with controllers that use the PRC described in Section 7. We present the results of a set of controllers that demonstrate our design process, going from a standard reference controller to a controller with that can easily change its power output and is refined for maximal power output using the modules described in this article. The simulation results, from DLC simulations, are discussed in terms of energy capture, maximum generator speeds, and structural loading.

First, we present a set of baseline controllers:

- NREL-5MW: The reference controller[21] commonly used as a benchmark for comparison in the wind turbine community
- BL-1.000: Our baseline for comparison, which includes the PI torque and pitch controllers (Section 4), set point smoothing controller (Section 5.1), and the PC (Section 5.2) with a constant PR $R = 1$.
- BL-1.050: Our "boosted" baseline, which is the same as the BL-1.000, but with an increased PI pitch control bandwidth ($\omega_{\text{reg},\theta} = 0.4\,\text{rad}\,\text{s}^{-1}$ vs. $0.275\,\text{rad}\,\text{s}^{-1}$), MPPS (Section 6), and only the slow PRC $PRC^{\,0}$ (Section 7.1) using a variable $R^{\max}$ up to 1.050, shown in Figure 6B. A WSE $\hat{u}_{\text{rot}}$ is used for the wind input.

The performance of these baseline controllers are compared with power reference controllers that make full use of the PRC in Section 7:

- PR-1.100: A controller with all of the previously described control modules, including the transient power reference control (PRC^1, Section 7.2) and a constant $R^{\max} = 1.100$, using a WSE $\hat{u}_{\text{rot}}$ for the wind signal and a PI pitch control bandwidth of $\omega_{\text{reg},\theta} = 0.275\,\text{rad}\,\text{s}^{-1}$.
- PR-1.150: The same as PR-1.100, but with an additional power boost below 18 $\text{m}\,\text{s}^{-1}$, up to $R^{\max} = 1.150$.

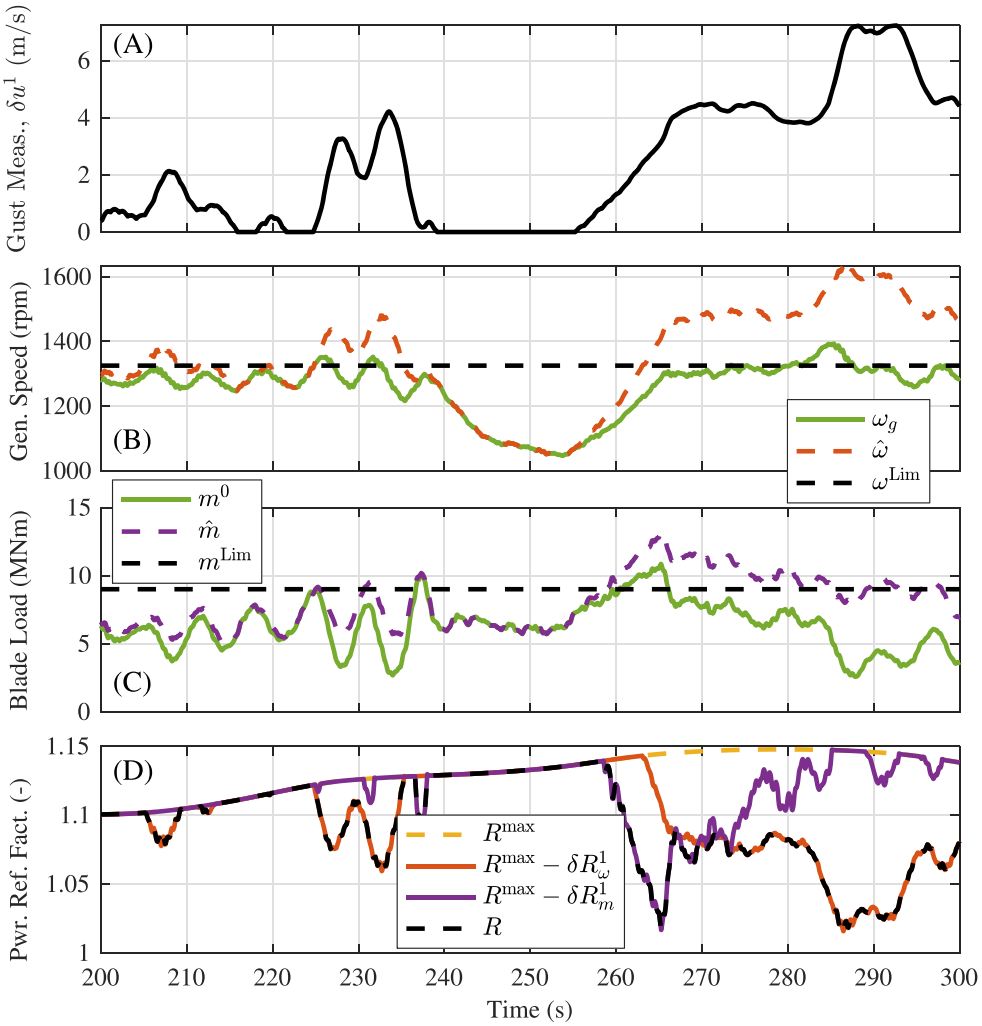

FIGURE 11 Demonstration of PRC^1. The gust measure δu^1 leads to transient estimates of the generator speed $\hat{\omega}$ and collective blade load $\hat{m}$. When the transient estimates exceed the limits ω^{Lim} or m^{Lim}, the transient de-rating signals δR^1_ω and δR^1_m reduce the power reference factor R from the maximum reference factor $R^{\max}$; these signals, also shown in Figure 8D, are used by the power controller

To measure the performance of the various controllers, we simulate each using the same set of wind fields defined in DLCs 1.2 and 1.3 (NTM and ETM, respectively). The full set of results are summarized in Table 5 in terms of the performance measures described in Section 2. Each controller is compared in terms of its energy capture (or lifetime average power) in both DLCs 1.2 and 1.3; an example for DLC 1.3 is shown in Figure 12D. The controllers are designed using a maximum generator speed constraint of 1408 rpm. In Figure 12A,B, the maximum generator speeds $\omega_g^{\max}$ are shown for each of the controllers.

The maximum blade loads are depicted in Figure 12C, while the maximum rotor thrust and blade loads are shown in Table 5. DLC 1.3 (ETM) is used to determine the generator speed, load, and thrust maxima and characteristic loading. DLC 1.2 is used to determine the tower base FA lifetime DEL for the various controllers. The lifetime average pitch travel (3) is determined using DLC 1.2 and is the primary cost of using the power regulator.

8.1 | Discussion of results

NREL-5MW and BL-1.000

The NREL-5MW reference controller results in a generator speed constraint violation during DLC 1.3 simulations ($\omega_g^{\max} = 1467$ rpm at 24 ms^{-1}, which exceeds the upper limit of 1408 rpm). Our baseline controller, BL-1.000, was tuned so that $\omega_g^{\max} < 1408$ rpm for all DLC 1.3 simulations and is used for comparison with all other controllers. The BL-1.000 has a lifetime average power within 1% of the NREL-5MW reference controller, while the maximum blade load and rotor thrust are reduced by 5.6% and 7.1%, respectively (Table 5).

TABLE 5 Summary of results for various controllers, detailing the energy capture, blade loads, rotor thrust, lifetime average pitch travel, maximum generator speed, and tower base fore-aft damage equivalent loading, with each measure (described in Section 2) compared to the BL-1.000 controller

	Lifetime average power (MW)		Blade load (MNm)	
Controller	**DLC 1.2**	**DLC 1.3**	**Characteristic**	**Maximum**
NREL-5MW Ref.	1834.6 (+0.61%)	2235.3 (+0.66%)	16.67 (+5.37%)	17.92 (+5.60%)
BL-1.000	1823.4 (-)	2220.6 (–)	15.82 (–)	16.97 (–)
BL-1.050	1837.6 (+0.78%)	2242.5 (+1.00%)	15.77 (−0.32%)	16.48 (−2.89%)
PR-1.100	1901.8 (+4.30%)	2328.0 (+4.84%)	15.55 (−1.71%)	16.59 (−2.24%)
PR-1.150	1925.4 (+5.60%)	2361.2 (+6.33%)	15.97 (+0.95%)	16.52 (−2.65%)
Controller	**Max. rotor thrust (MN)**	**Pitch travel ($^\circ$ s^{-1})**	**Max. gen. speed (rpm)**	**Tower base fore-aft DEL (MNm)**
NREL-5MW Ref.	1.02 (+4.45%)	0.1386 (+24.5%)	1467	20.8 (−9.17%)
BL-1.000	0.977 (–)	0.1113 (–)	1402	22.9 (–)
BL-1.050	0.978 (+0.54%)	0.1566 (40.7%)	1384	25.6 (+11.8%)
PR-1.100	0.909 (−7.00%)	0.2121 (+90.6%)	1399	21.5 (−6.11%)
PR-1.150	0.964 (−1.31%)	0.2046 (+83.8%)	1406	23 (+0.43%)

Note: The maximum allowable generator speed limit is 120% of the nominal rated generator speed or 1408 rpm.

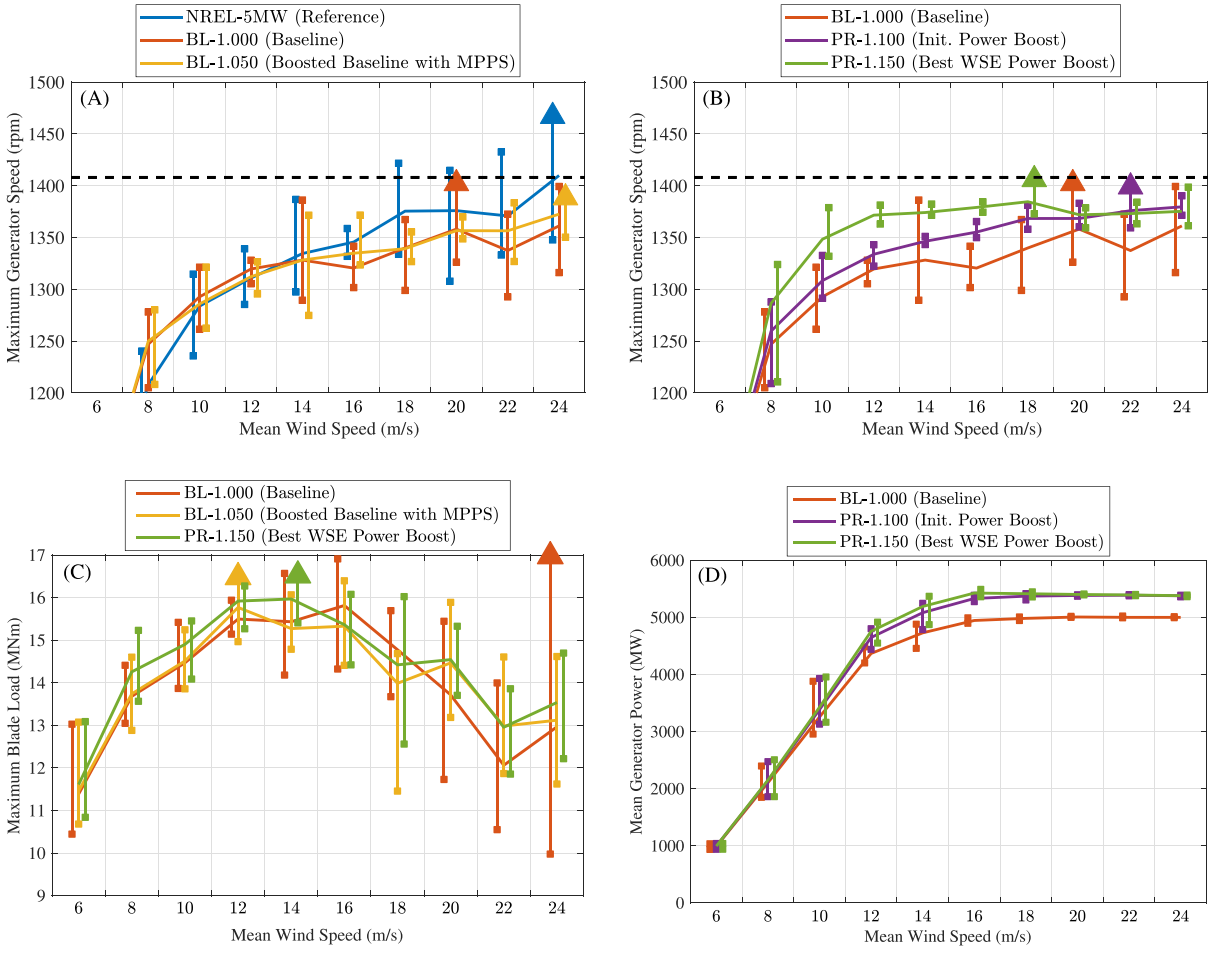

FIGURE 12 Maximum generator speeds (A,B), maximum blade loads (C), and average generator power (D) for the various controllers described in Section 8. At each mean wind speed, the maximum generator speeds, maximum blade loads, and mean generator power of six turbulent wind simulations span the vertical lines between the squares (■); the overall maxima is denoted with a triangle (▲). Note that the vertical lines are offset horizontally for comparison purposes

BL-1.050

If we increase the bandwidth of the PI pitch controller via ω_{reg} (from 0.275 to 0.4 rad s^{-1}), as we do for the BL-1.050, the generator speed has less variation (and overshoot) from its set point and we are able to boost the PR up to $R^{\max} = 1.050$. Based on our stability analysis (Section 7.3.1), the increased PI pitch gains reduce the stability margin; thus, we could not use the transient PRC with the BL-1.050 controller. To decrease blade loads (especially at high wind speeds), we must include the minimum pitch control; notice, in Figure 12C, that the maximum blade load for the baseline (BL-1.000) control occurs near cut-out. The steady power regulator must also be used to decrease $R^{\max}$ near-rated wind speeds. Otherwise, an ETM simulation at 14 m s^{-1} has a generator speed peak that exceeds 1408 rpm. Compared with the BL-1.000 controller, the BL-1.050 increases the lifetime average power by 1%, lifetime average pitch travel by 41%, and the tower base FA DEL by 12%, while there is only a small change in the other performance measures.

PR-1.100 and PR-1.150

The transient PRC (PRC^{1}) (with the original PI pitch controller using $\omega_{\text{reg}} = 0.275$ rad s^{-1}) allows us to increase $R^{\max}$ because of the reduced spread in $\omega_g^{\max}$, compared to the baselines, as shown in Figure 12A,B. PR-1.100 increases the lifetime average power by 4% compared to the baseline, but there is a gap between the maximum generator speeds below 18 ms^{-1} and the hard upper bound, which implies that $R^{\max}$ can be increased even more at these wind speeds. Thus, the slow power reference control (PRC^{0}) can be used to increase $R^{\max}$ more below 18 ms^{-1}, resulting in the largest amount of power boost achieved (using a WSE and other control modules described in this article) that satisfies all the constraints. Compared to the BL-1.000, the PR-1.150 increases lifetime average power by 5.6% during DLC 1.2 and 6.3% in DLC 1.3. This increase in power must be balanced with a notable increase in blade pitch travel (83.8%), either by upgrading pitch bearings or accounting for their damage over time.

9 | CONCLUSIONS

In this article, we present a controller that increases energy capture while maintaining the same generator speed and blade load limits. Because AEP has a direct impact on the LCOE, while loads and generator speed behave more like constraints on the overall design, we believe these goals more accurately reflect system-level turbine design goals.

We achieve these goals by increasing the power reference and then de-rating (or decreasing) the PR only when a critical performance variable would otherwise exceed some threshold. In this article, we control peak transients in the generator speed and flapwise blade loads, though the method could be applied more generally to other loads or values. This power reference control was implemented and analyzed using a hybrid controller, which interacts with a series of modular control elements, reflecting collaborative design practices and allowing control engineers to utilize the various modules we have presented. The PRC provides an input to a PC, which reduces generator speed and blade load transients while increasing power output. Peak load shaving is implemented using a minimum pitch limit. An SPC determines the generator speed set points to provide minimal interaction between the PI pitch and torque controllers, which supply the direct inputs to the turbine.

Using the power reference controller with a wind speed estimate increases lifetime average power by 5%–6% compared to a baseline controller with a constant PR. Generator speeds stay below a pre-defined threshold, peak blade loads are reduced, and tower fatigue increases by less than 1%. However, designers must balance the control benefits presented in this article with an 84% increase in pitch travel. By reconsidering our control goals and aligning them with the system-level goals of wind turbine design, we can improve performance from a system-level perspective.

ACKNOWLEDGEMENTS

The information, data, and work presented herein was funded in part by the Advanced Research Projects Agency - Energy (ARPA-E), US Department of Energy, under Award DE-AR0000667. Support from a Palmer Endowed Chair Professorship is also gratefully acknowledged. The views and opinions of the authors expressed herein do not necessarily state or reflect those of the United States Government or any agency thereof.

PEER REVIEW

The peer review history for this article is available at https://publons.com/publon/10.1002/we.2705.

DATA AVAILABILITY STATEMENT

The data that support the findings of this study are available from the corresponding author upon reasonable request.

ORCID

Daniel S. Zalkind https://orcid.org/0000-0003-0482-3285

REFERENCES

1. Stehly T, Beiter P, Heimiller D, Scott G. 2017 Cost of wind energy review. NREL/TP-5000-63267, National Renewable Energy Laboratory; 2018. https://www.nrel.gov/docs/fy18osti/72167.pdf
2. Zalkind DS, Ananda GK, Chetan M, et al. System-level design studies for large rotors. *Wind Energy Sci*. 2019;4(4):595-618. https://doi.org/10.5194/wes-4-595-2019
3. Pao LY, Zalkind DS, Griffith DT, et al. Control co-design of 13MW downwind two-bladed rotors to achieve 25% reduction in levelized cost of wind energy. *Annu Rev Control*. 2021;51:331-343. https://doi.org/10.1016/j.arcontrol.2021.02.001
4. Bortolotti P, Bottasso CL, Croce A. Combined preliminary–detailed design of wind turbines. *Wind Energy Sci*. 2016;1(1):71-88. https://doi.org/10.5194/wes-1-71-2016
5. Jonkman JM, Buhl ML. FAST user's guide. NREL/TP-500-38230, National Renewable Energy Laboratory; 2005. https://github.com/openfast/openfast
6. Hansen MH, Henriksen LC. Basic DTU wind energy controller. E-0018, Technical University of Denmark; 2013. https://orbit.dtu.dk/files/56263924/DTU_Wind_Energy_E_0028.pdf
7. Abbas N, Zalkind D, Pao L, Wright A. A reference open-source controller for fixed and floating offshore wind turbines. *Wind Energy Sci Discuss*. 2021:1-33. https://doi.org/10.5194/wes-2021-19
8. Bossanyi EA. Wind turbine control for load reduction. *Wind Energy*. 2003;6(3):229-244. https://doi.org/10.1002/we.95
9. Aho J, Buckspan A, Laks J, et al. A tutorial of wind turbine control for supporting grid frequency through active power control. In: 2012 American Control Conference (ACC); 2012; Montreal, QC, Canada:3120-3131.
10. Siemens Wind Power. Siemens power boost function. online. http://www.energy.siemens.com/us/pool/hq/services/renewable-energy/wind-power/swp-power-boost-function.pdf; 2014.
11. Vestas Wind Systems. Vestas launches new upgrades to increase output of installed turbines. online. https://www.vestas.com/en/media/∼/media/dd6c48580743401b8710fa22cc9c68e5.ashx; 2014.
12. Petrović V, Bottasso CL. Wind turbine envelope protection control over the full wind speed range. *Renew Energy*. 2017;111:836-848.
13. Kanev S. Extreme turbulence control for wind turbines. *Wind Eng*. 2017;41. https://doi.org/10.1177/0309524X17723204
14. Henzinger TA. The theory of hybrid automata. In: Proceedings 11th Annual IEEE Symposium on Logic in Computer Science; 1996; New Brunswick, NJ, USA:278-292.
15. Zalkind DS, Pao LY. Constrained wind turbine power control. In: 2019 American Control Conference (ACC); 2019; Philadelphia, PA, USA:3494-3499.
16. Zalkind DS. Methods for enabling control collaboration during wind turbine design. *Ph.D. Thesis*. Boulder, CO, USA; 2020. https://search.proquest.com/openview/27a2025fed70d7a2e0218253fe977c3e/1?pq-origsite=gscholar&cbl=18750&diss=y
17. International Electrotechnical Commission. Wind turbines—part 1: design requirements. IEC 61400-1:2005(E); 2005.
18. Griffith DT, Richards PW. The SNL100-03 blade: design studies with flatback airfoils for the Sandia 100-meter blade. SAND2014-18129, Sandia National Laboratory; 2014. http://energy.sandia.gov/wp-content/gallery/uploads/dlm_uploads/1418129.pdf
19. Ning A, Damiani R, Moriarty PJ. Objectives and constraints for wind turbine optimization. *J Solar Energy Eng*. 2014;136(4):041010.
20. Hayman GJ. MLife theory manual for version 1.00. NREL/TP-XXXXX, National Renewable Energy Laboratory; 2012. https://nwtc.nrel.gov/system/files/MLife_Theory.pdf
21. Jonkman JM, Butterfield S, Musial W, Scott G. Definition of a 5-MW reference wind turbine for offshore system development. NREL/TP-500-38060, National Renewable Energy Laboratory; 2009. https://www.nrel.gov/docs/fy09osti/38060.pdf
22. NREL. Openfast. Version 2.2.0. Online. https://github.com/OpenFAST/openfast; 2019.
23. Jonkman BJ, Kilcher L. TurbSim user's guide: version 1.06.00. TP-500-39797, National Renewable Energy Laboratory; 2012. https://nwtc.nrel.gov/system/files/TurbSim.pdf
24. Dunne F, Aho J, Pao LY. Analysis of gain-scheduling implementation for the NREL 5-MW turbine blade pitch controller Proc. American Control Conference; 2016:3188-3193.
25. Zalkind DS, Dall'Anese E, Pao LY. Automatic controller tuning using a zeroth-order optimization algorithm. *Wind Energy Sci*. 2020;5(4):1579-1600. https://wes.copernicus.org/articles/5/1579/2020/
26. Schlipf D. Controller design and implementation. TTI GmbH - Sowento TGU. https://doi.org/10.5281/zenodo.5567358; 2019.
27. Simulink. Simulation and model-based design. MathWorks. https://www.mathworks.com/products/simulink.html; 2020.
28. Vidyasagar M. *Nonlinear systems analysis*. 2nd ed. Englewood Cliffs: Prentice Hall; 1993.
29. Knudsen T, Bak T, Soltani M. Prediction models for wind speed at turbine locations in a wind farm. *Wind Energy*. 2011;14(7):877-894. https://doi.org/10.1002/we.491
30. Simley E, Pao LY. Evaluation of a wind speed estimator for effective hub-height and shear components. *Wind Energy*. 2016;19(1):167-184. https://doi.org/10.1002/we.1817
31. Bar-Shalom Y, Li XR, Kirubarajan T. *Estimation with Applications to Tracking and Navigation*. USA: John Wiley & Sons, Inc; 2002.
32. Soltani MN, Knudsen T, Svenstrup M, Wisniewski R, Brath R, Ortega R, Johnson K. Estimation of rotor effective wind speed: a comparison. *IEEE Trans Control Syst Technol*. 2013;21(4):1155-1167. https://doi.org/10.1109/TCST.2013.2260751

How to cite this article: Zalkind DS, Nicotra MM, Pao LY. Constrained power reference control for wind turbines. *Wind Energy*. 2022;25(5):914-934. doi:10.1002/we.2705

APPENDIX A: WIND SPEED ESTIMATOR

The output of a WSE is used in multiple control modules described in this article:

- In Section 6, a low-pass filtered WSE is used to determine the lower limit of the pitch controller during near- and above-rated operation for peak load reduction,
- In Section 7.1, a filtered WSE is used to change the maximum allowable PR, and
- In Section 7.2, the WSE is translated into a gust measure that is used to estimate problematic transients and de-rate the turbine from the maximum allowable PR.

Using known inputs and outputs of the turbine, the WSE provides an estimated wind speed signal. The WSE in this article is implemented as a discrete EKF, with state dynamics for the drivetrain and mean and turbulent wind speed dynamics. The drivetrain degree-of-freedom is primarily driven by the power coefficient, which is estimated from sampled simulation data.[16] The wind speed dynamics include a slowly varying mean wind speed and a quickly varying turbulent component, which combine to provide the WSE.[29] A discrete EKF provides a simple implementation; similar examples[30,31] and additional details of the WSE used in this article are provided in previous work.[16]

An example WSE is shown in Figure 9, which is used to estimate transients in Figure 11, and also set the maximum PR in Figure 8D and minimum pitch angle in Figure 8A. Overall performance measures of the WSE used in this article are provided in previous work.[16] The goal was to design a WSE with low bias, for accurately determining the operating wind speed, and one with adequate disturbance estimation, measured via the relative degree of explanation (RDE).[32] Our WSE has RDE values greater than 75% across the operating wind speeds, which provides the controller with adequate disturbance estimation; it is not necessarily the best WSE possible but was used to attain the results in this article.